WCCM V
Fifth World Congress on
Computational Mechanics
July 7–12, 2002, Vienna, Austria
Eds.: H.A. Mang, F.G. Rammerstorfer,
J. Eberhardsteiner

On strategies for tracking strong discontinuities in computational failure mechanics

J. Oliver*

E.T.S. d'Enginyers de Camins, Canals i Ports
Universitat Politècnica de Catalunya (UPC),
Campus Nord UPC, Edifici C-1 C/ Gran Capitán s/n
08034 Barcelona Spain
e-mail: oliver@cimne.upc.es

A. E. Huespe

CIMEC/CONICET-UNL
Santa Fe, Argentina
e-mail: ahuespe@intec.unl.edu.ar

E. Samaniego*, **and E.W.V. Chaves***

Key words: strong discontinuities, tracking, heat conduction

Abstract
The work deals with the strategies for tracking displacement jumps (strong discontinuities) in computational failure mechanics in the context of finite elements with embedded discontinuities. As an alternative to classical strategies, based on the spatial propagation of a selected discontinuity, a new technique is presented. The strategy lies on tracing, at once, the envelope family of the propagation directions all over the domain and, then, select the one (or the ones) of interest. The mathematical problem is presented in terms of a heat-conduction like problem, which facilitates the physical perception of the results and the understanding of the numerical difficulties. Numerical examples and application to fracture problems are presented.

1 Introduction

Numerical simulation in failure mechanics has been enriched in the last years by new technologies to capture discontinuities in the displacement fields, which are more technically termed *strong discontinuities* [13], [8]. A very important ingredient in modelling the appearance and development of those strong discontinuities is the algorithm that identifies the locus of material points along which the discontinuities proceed i.e.: the *discontinuity paths* that, depending on the context, are termed cracks, fracture lines, shear bands, slip lines, etc.

In many modelling strategies, the discontinuity paths have to be precisely identified in order to succeed in the analysis. This is the case of some finite elements with embedded discontinuities [3], [4], [12], [7], [9], [1], [11] and the extended finite element method [2], [14] where the selection of the deformation modes capturing the displacement jumps crucially lies on the way that the element is crossed by the discontinuity. Those strategies devoted to predicting and capturing the geometrical position inside the body (and in the context of a finite element analysis inside every finite element) of those discontinuity paths will be termed, from now on, *tracking strategies.*

This work is devoted to analyzing some of the existing strategies for tracking strong discontinuities as well as to exploring some alternatives that could offer a better performance in terms of robustness and simplicity of implementation in the context of multifracturing problems.

2 Tracking strong discontinuities

For the sake of simplicity we shall consider first the two-dimensional case. Let us consider a 2D body Ω, liable to experience strong discontinuities. Let us denote the corresponding discontinuity paths by $\mathcal{S}_i$ $i \in \{1, ...n_d\}$ where n_d is the number of them (see figure 1-(a)).

In the following we shall assume that the input data for the algorithm provides:

1) A *condition for propagation* of the discontinuity. In the simplest cases this condition signals the end of the elastic regime in the bulk through the fulfillment of some yield or damage criterion [15]. For some more sophisticated cases, propagation can be triggered after the elastic regime when bifurcation criteria (loss of strong ellipticity) are fulfilled [10], [8].

2) A *direction of propagation.* This direction is given either on empirical basis (for instance, the propagation direction is considered orthogonal to the maximum tensile stress) or it is supplied by more sophisticated local bifurcation analyses (for instance, the propagation direction is the one providing the first possible bifurcation of the stress-strain field) [10], [8].

In any case we shall assume that at any point $\mathbf{x}$ of the body and at any time t of the analysis, a vector field $\mathbf{T}(\mathbf{x},t)$, signaling the direction of propagation of a discontinuity path having its tip at $\mathbf{x}$, is available. In the context of a finite element analysis we assume that there is one available $\mathbf{T}^{(e)}$ for every sampling point inside the element e (see figure 1-(b)).

In this context we can envisage two possible strategies for tracing the active discontinuities at a given time of the analysis:

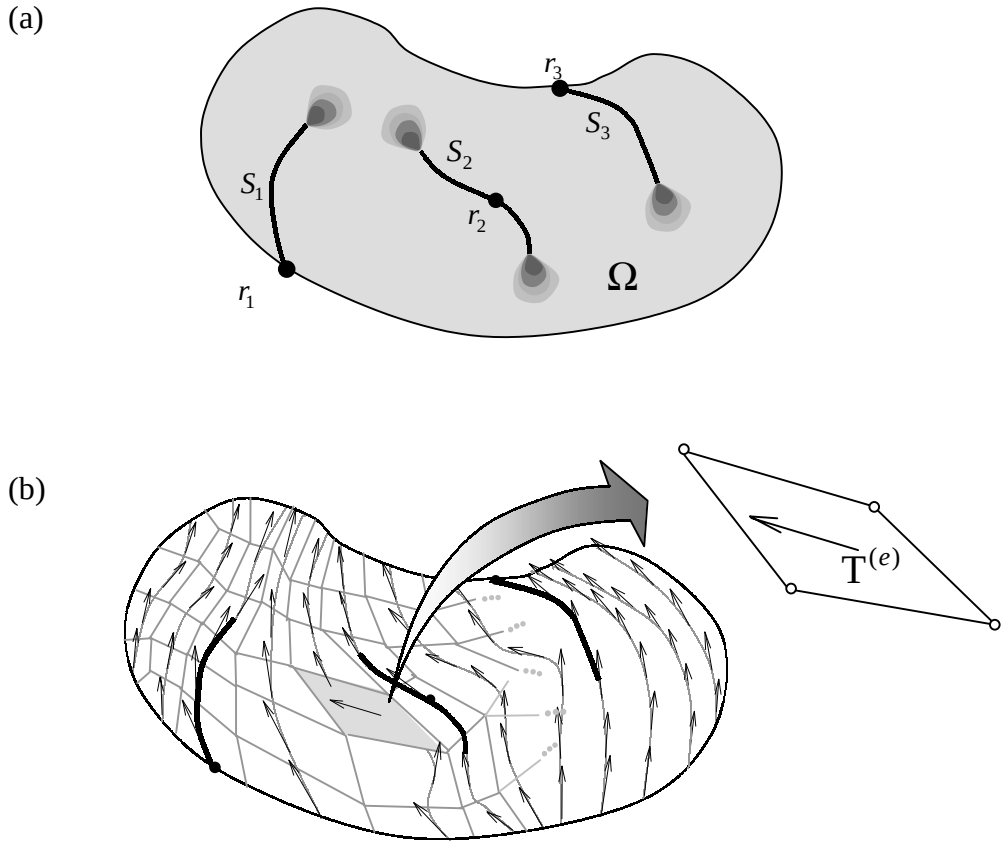

Figure 1: Discontinuity paths in a body.

A) *LOCAL TRACKING.* This strategy is based on the local propagation of the discontinuity and lies on the following ingredients:

1) *Propagation of an existing discontinuity S_i from its root*, see figure 1-(a) (in the context of a sequential time analysis, the discontinuity line root r_i is the material point, or the finite element, at which the discontinuity S_i is triggered off). That propagation can be made through the following geometrical algorithm (see also figure 2) at elemental level:

DATA:	Discontinuity input point I_{S_i} Propagation direction $\mathbf{T}^{(e)}$
ACTIONS:	
1)	Trace a line in direction $\mathbf{T}^{(e)}$ passing through I_{S_i}
2)	Find the intersected output point O_{S_i}
3)	Consider the geometrical position of O_{S_i} as the input discontinuity I_{S_i} point for the neighbour element e+1.

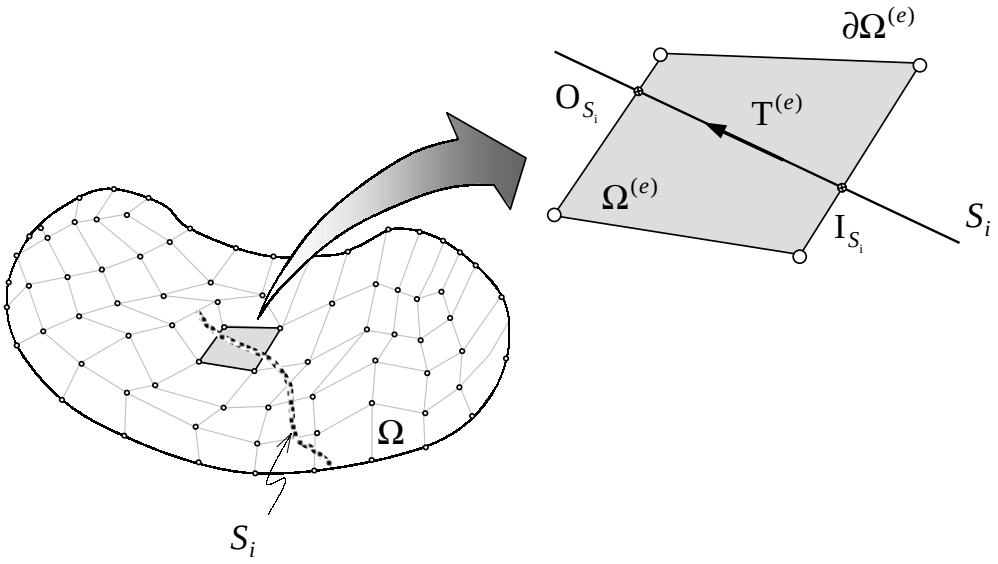

Figure 2: Local tracking of a discontinuity.

Indeed, the algorithm requires handling of a *side-connectivity array* signaling those elements that share their sides with a given one.

2) *Identification of the root*, r_i of a new discontinuity path S_i (see figure 1-(a)). Any element e, satisfying for the first time the propagation condition above, is declared the root r_{n_d}, of a new discontinuity line S_{n_d}, whenever there is no discontinuity input point I_{S_i} $i \in \{1, ..., n_d - 1\}$ placed on its boundary $\partial\Omega^{(e)}$ (see figure 2).

This strategy is quite simple, robust and reliable when dealing with a single discontinuity line, and it has been fairly successful in the past [9], [5], [6]. However, in case of consideration of many discontinuity lines (multifracture) it can lose much of its robustness.

B) *OVERALL (GLOBAL) TRACKING.*

As an alternative to the previous strategy one could consider the one based on the following steps:

1) *Trace at once all the possible discontinuity paths* ad time t. Since, by construction, at every point $\mathbf{x}$ of the discontinuity lines S_i, the tangent has the sense of the propagation vector $\mathbf{T}(\mathbf{x},t)$, then the S_i are segments of the family of curves enveloping the vector field $\mathbf{T}$ (see figure 1). Therefore, the construction of the envelopes implicitly supplies all the possible discontinuity lines at time t. These envelopes can be described by a function $\theta(\mathbf{x})$ whose *level contours* ($\theta(\mathbf{x})$ =constant) define all the possible discontinuity lines as (see figure 3):

$$S_i := \{\mathbf{x} \in \Omega \,;\, \theta(\mathbf{x}) = \theta_{S_i}\} \tag{1}$$

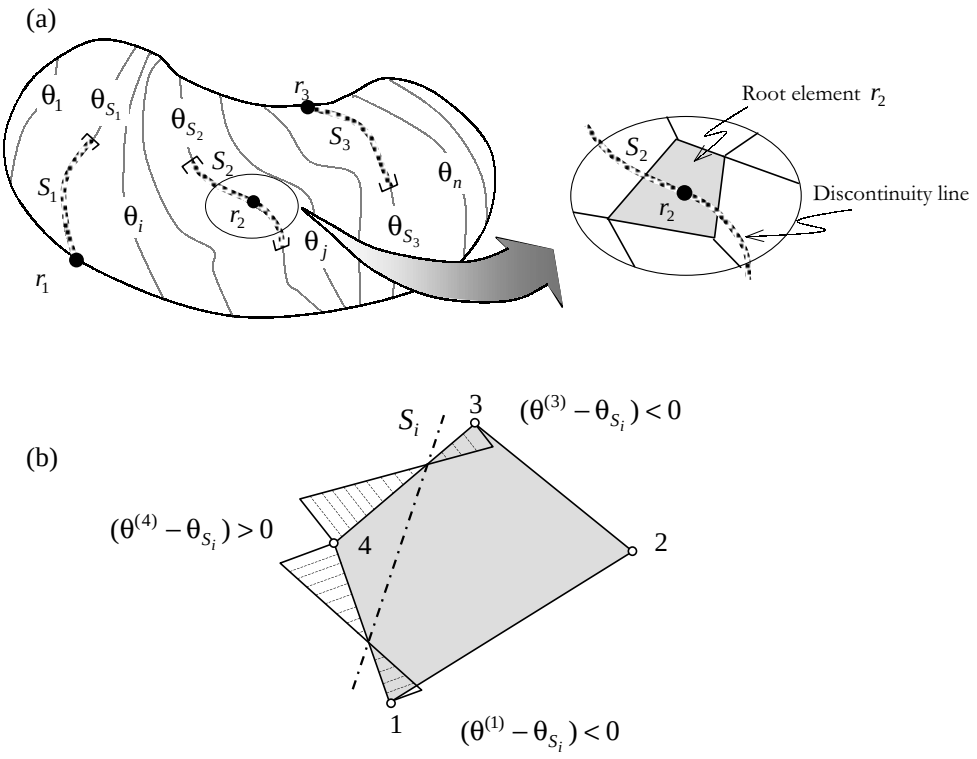

Figure 3: Global tracking of discontinuities

for all the meaningful values of θ_{S_i} and for all the material points, $\mathbf{x}$, fulfilling the propagation condition. In section (3) a methodology for construction of such a family is provided were $\theta(\mathbf{x})$ stands for the temperature field that is the solution of a stationary heat conduction problem and, therefore, S_i are segments of the isothermal lines. In the context of a finite element analysis, this algorithm returns the nodal temperature values $\theta^{(k)}$.

2) *Identify the active discontinuity lines and their corresponding temperature level.* For every root element r_i, it is considered that the discontinuity path passes through its centroid (see figure 3-(a)). Consequently, the corresponding temperature level is the average of the nodal temperatures for this root element:

$$\theta_{S_i} = \frac{1}{n} \sum_{k=1}^{n} \theta^{(k)} \tag{2}$$

where n stands for the number of nodes of the element (i.e.: $n = 3$, for linear triangles and $n = 4$ for linear quadrilaterals). Then, temperatures θ_{S_i} $i = 1, ..n_d$ identify the corresponding discontinuity lines S_i through equation (1).

3) *Determine the position of the discontinuity line inside a given element.* Once the nodal temperatures $\theta^{(k)}$ and the discontinuity line temperatures θ_{S_i} are known, the position of S_i inside a given element e can be immediately determined through the following algorithm

(see figure 3-(b)):

DATA:	Nodal temperatures of the element: $\theta^{(k)}$ Discontinuity line temperature: θ_{S_i}
ACTIONS:	
1)	Determine the sides involving a change of sign of $(\theta^{(k)} - \theta_{S_i})$ at their vertices (sides crossed by S_i).
2)	For every of these sides compute the position of S_i through linear interpolation.

(3)

Notice that no information from the neighbour elements is required in the preceding algorithm. This fact confers to the algorithm some interesting locality character that can be exploited for implementation purposes.

4) *Identification of the root*, r_i of a new discontinuity path S_i . Any element e, satisfying for the first time the propagation condition, is declared the root r_{n_d}, of a new discontinuity line S_{n_d}, whenever it is not crossed by any discontinuity line S_i $i \in \{1, ..., n_d - 1\}$ according to the previous algorithm.

3 Enveloping of the propagation vector field

Let us now focus on a procedure to compute the envelopes of a vector field $\mathbf{T}(\mathbf{x})$ in a two-dimensional domain Ω. We shall assume that $\mathbf{T}(\mathbf{x})$ is a unit vector field, i.e.:

$$\mathbf{T} \cdot \mathbf{T} = \|\mathbf{T}\|^2 = 1 \tag{4}$$

whose sense shall be not relevant. The final goal is to obtain a function $\theta(\mathbf{x})$ whose level lines, defined by equation (1), are envelopes of $\mathbf{T}$. Since those contours are orthogonal to the gradient, function $\theta(\mathbf{x})$ shall be the solution of the following partial differential equation:

$$\mathbf{T} \cdot \nabla\theta = \nabla\theta \cdot \mathbf{T} = \frac{\partial\theta}{\partial T} = 0 \qquad in\ \ \Omega \tag{5}$$

where $\frac{\partial\theta}{\partial T}$ stands for the directional derivative (in the direction of $\mathbf{T}$) of θ.

3.1 Heat conduction-like problem

Multiplying equation (5) times $\mathbf{T}$ we obtain:

$$\begin{aligned} &\mathbf{T}\frac{\partial\theta}{\partial T} = (\mathbf{T} \otimes \mathbf{T}) \cdot \nabla\theta = \mathbb{K}{\cdot}\nabla\theta \\ &\mathbb{K} := \mathbf{T} \otimes \mathbf{T} \end{aligned} \tag{6}$$

Now defining:

$$\mathbf{q} = -\mathbb{K}{\cdot}\nabla\theta \tag{7}$$

we consider the following boundary value problem:

$$\begin{array}{lll} FIND: \theta(\mathbf{x}) & \text{satisfying:} & \\ \nabla \cdot \mathbf{q} = 0 & in\ \ \Omega & (a) \\ \mathbf{q} = -\mathbb{K}\cdot\nabla\theta = -\mathbf{T}\frac{\partial\theta}{\partial T} & in\ \ \Omega & (b) \\ \mathbf{q}\cdot\nu = (\nu\cdot\mathbf{T})\frac{\partial\theta}{\partial T} = 0 & on\ \ \partial_q\Omega & (c) \\ \theta = \theta^* & on\ \ \partial_\theta\Omega & (d) \end{array} \tag{8}$$

where ν is the outward normal to the boundary $\partial\Omega$ and $\partial_q\Omega$ and $\partial_\theta\Omega$ ($\partial_q\Omega \cup \partial_\theta\Omega = \partial\Omega$) stand, respectively, for the parts of the boundary $\partial\Omega$ were Newman and Dirichlet conditions are prescribed.

If the Dirichlet boundary conditions (8)-(d) are compatible with condition $\frac{\partial\theta}{\partial T} = 0$ then a solution satisfying:

$$\theta(\mathbf{x}) \neq constant \quad ; \quad \frac{\partial\theta}{\partial T} = 0 \tag{9}$$

is a solution of problem (8) as can be checked by substitution of equation (9) in equations (8). In other words, that solution of problem (8) will provide a solution of the original partial differential equation and, thus, the corresponding envelopes (1).

Problem (8) can be regarded as the steady-state heat conduction equation in Ω (see figure 4), for the case of no internal heat sources and null heat flux input ($q_\nu = \mathbf{q}\cdot\nu = 0$) in the boundary $\partial_q\Omega$ (adiabatic boundary). In this case θ plays the role of the temperature field, $\mathbf{q}$ is the conduction flux vector and $\mathbb{K}$ is a, point dependent, anisotropic thermal conductivity tensor given by:

$$[\mathbb{K}(\mathbf{T}(\mathbf{x}))] = [\mathbf{T}\otimes\mathbf{T}] = \begin{bmatrix} T_x^2 & T_xT_y \\ T_xT_y & T_y^2 \end{bmatrix} \tag{10}$$

Remark 1: Notice that $\mathbb{K}(\mathbf{T}) = \mathbb{K}(-\mathbf{T})$) and, as expected, the solution of problem (8) is only affected by the direction of the vector field $\mathbf{T}$ and not by its sense.

Remark 2: The rank-one character of the conductivity tensor (10) can be source of ill-posedness of the heat conduction problem (8). Indeed, since the flux vector $\mathbf{q}$, in equation (8)-(b), has a null component in the direction $\mathbf{N}$ orthogonal to $\mathbf{T}$, from equation (9) the value of the directional derivative $\frac{\partial\theta}{\partial N} := \nabla\theta\cdot\mathbf{N}$ is not determined and the evolution of the solution of the problem, $\theta(\mathbf{x})$, in the direction of $\mathbf{N}$ is undefined. In order to overcome the extra singularity problems associated to this fact in numerical simulation settings, the conductivity tensor (10) is modified as follows:

$$\mathbb{K}_\epsilon = \mathbf{T}\otimes\mathbf{T} + \epsilon\mathbf{1} \tag{11}$$

where $\mathbf{1}$ is the unit tensor and ϵ[1] is an isotropic algorithmic conductivity, small enough to fulfill, for practical purposes, equation (9) but sufficiently large to break down the singularity of $\mathbb{K}$.

[1] In the numerical simulations below a value of $\epsilon = 10^{-6}$ has been considered.

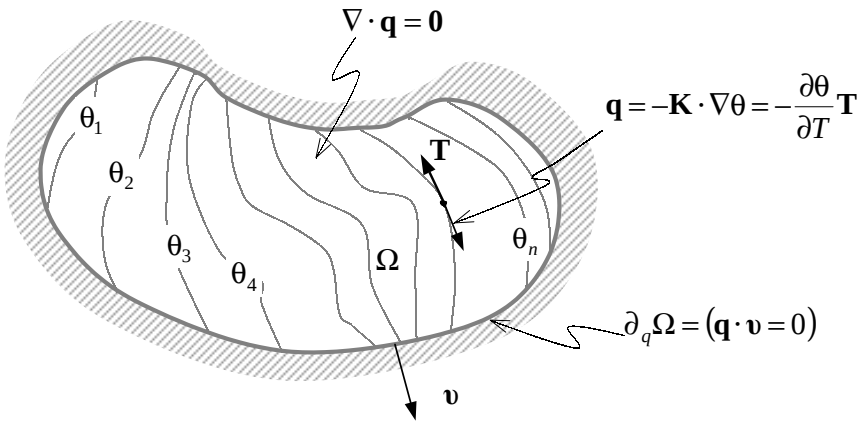

Figure 4: Stationary heat conduction problem.

3.2 Finite element formulation:

Given a finite element discretization of Ω, with n_{elem} elements and n_{node} nodes the discrete counterpart of the continuum problem (8) follows from standard procedures [17]. It can be summarized as follows:

FIND:

$$\theta^h(\mathbf{x}) = \Sigma_{i=1}^{i=n_{node}} \; N_i\theta_i \quad = [\mathbf{N}]^T \cdot [\theta] \qquad ; \quad \theta_i|_{\partial_\theta\Omega} = \theta^*$$

$$\left\{ \begin{array}{l} [\mathbf{N}] := [N_1, ..., N_{n_{node}}]^T \\ [\theta] := [\theta_1, ..., \theta_{n_{node}}]^T \end{array} \right. \tag{12}$$

SUCH THAT:

$$\begin{array}{l} \mathbf{K} \cdot \theta = \mathbf{0} \\ \theta_i|_{\partial_\theta\Omega} = \theta^* \\ \mathbf{K} = \int_\Omega [\nabla\mathbf{N}]^T \, [\mathbb{K}_\epsilon] \, [\nabla\mathbf{N}] \, d\Omega \end{array} \tag{13}$$

where $N_i(\mathbf{x})$ are the standard shape functions and $\mathbf{K}$ is the resulting stiffness matrix. Equations (13) define a linear thermal problem that has to be solved at the beginning of every time step of the original mechanical problem, this providing the required position of the discontinuity paths inside the finite element mesh according to the algorithm in equation (3).

If there is no prescribed temperature ($\partial_\theta\Omega = \emptyset \Rightarrow \partial_q\Omega = \partial\Omega$) then the rank of $\mathbf{K}$ is $n_{node} - 1$. Thus, the temperature has to be prescribed at, at least, one node in order to provide a unique solution of system (13). In addition, in order to preclude solutions of the type θ =constant (which would not distinguish the different isothermal lines) the temperature should be prescribed at one additional node. The values of the prescribed temperatures are irrelevant for the goal of the model whenever they are not imposed on two points of the same isothermal line.

4 Representative numerical simulations

The set of simulations shown in figure 5 illustrates the performance of the heat conduction model presented above, to trace envelopes of arbitrary vector fields.

The considered square domain is discretized by means of the unstructured finite element mesh of quadrilaterals shown in figure 5-(a). Figures 5-(b) to (d) show different vector fields (left) and the corresponding contours of iso-temperatures (right) obtained with that model. For every case, the two nodal points with prescribed temperatures are shown. It is worth noting that, disregard the character of the vector field, the envelops are precisely captured even if their direction changes abruptly (see figure 5-(d)).

The methodology outlined in previous sections is then applied for computational failure mechanics purposes. In figure 6 the classical four points bending test [16] on a concrete specimen is sketched. The fracture process is modeled by means of the strong discontinuity approach described by the authors in [6] and the numerical simulation is made on the basis of the unsymmetrical finite element with embedded discontinuities described in [9].

A continuum Rankine type plasticity model, equipped with strain softening, is used to provide the required ingredients to trigger and propagate the crack as a regularized strong discontinuity. On the basis of this model, the discontinuous bifurcation analysis [10] results in the maximum (tensile) principal stress direction as the most critical for propagation of the discontinuity.

The heat conduction algorithm of section 3 is used, at every time step of the analysis, to trace the possible candidates to discontinuity paths and, then, the algorithm in equation (3) determines the actual position of the discontinuity inside every element.

In figure 6-(a) the geometrical and loading features of the problem are sketched together with the considered finite element mesh, of four noded quadrilaterals. Figure 6-(b) shows, at the first (elastic) time step of the analysis and for the central part of the beam, the first principal stress distribution (left) and the corresponding envelopes (right). Finally, in figure 6-(c) the final cracks (darkened) predicted by the simulation are presented (left) together with the final envelopes of the first principal stress (right).

5 Generalization to 3D cases

Generalization, from the 2D case considered above, to the general 3D case follows trivially. Let $\mathbf{N}(\mathbf{x},t)$ be a family of unit vectors, defined at every point in the domain Ω at a given time t,determining the direction normal to the the plane of propagation of the discontinuity. Then, let $\mathbf{S}(\mathbf{x},t)$ and $\mathbf{T}(\mathbf{x},t)$ be any couple of unit vectors orthogonal to $\mathbf{N}$ so that:

$$\mathbf{S}\cdot\mathbf{N} = \mathbf{T}\cdot\mathbf{N} = 0 \tag{14}$$

thus defining the plane (tangent to them) of propagation of the discontinuity. The family of surfaces, enveloping both vectors, $\mathbf{S}$ and $\mathbf{T}$, can be described by a scalar (temperature like) function $\theta(\mathbf{x})$ such that the isothermal surfaces:

$$S_i := \{\mathbf{x} \in \Omega \,;\, \theta(\mathbf{x}) = \theta_{S_i}\} \tag{15}$$

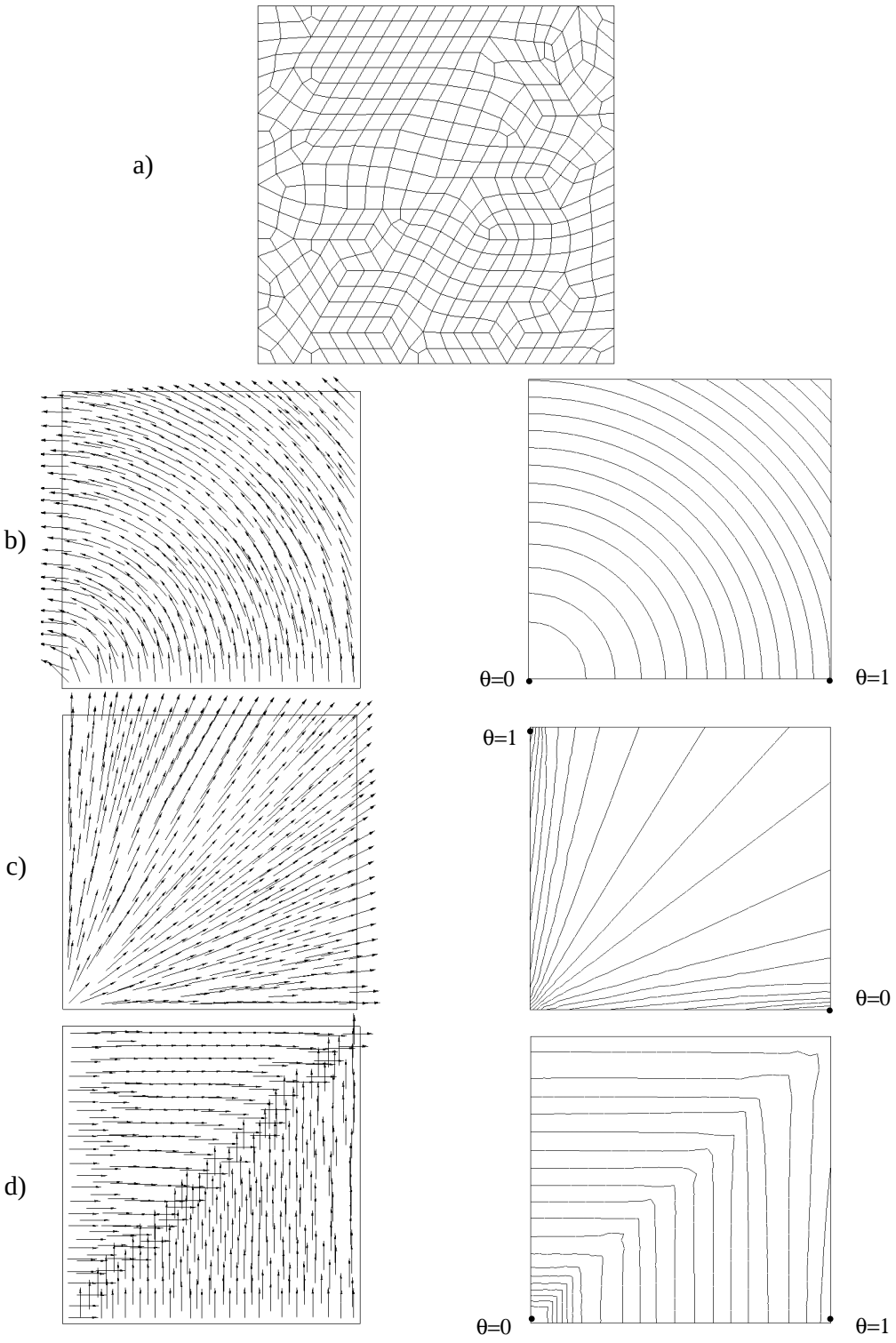

Figure 5: Envelopes of vector fields.

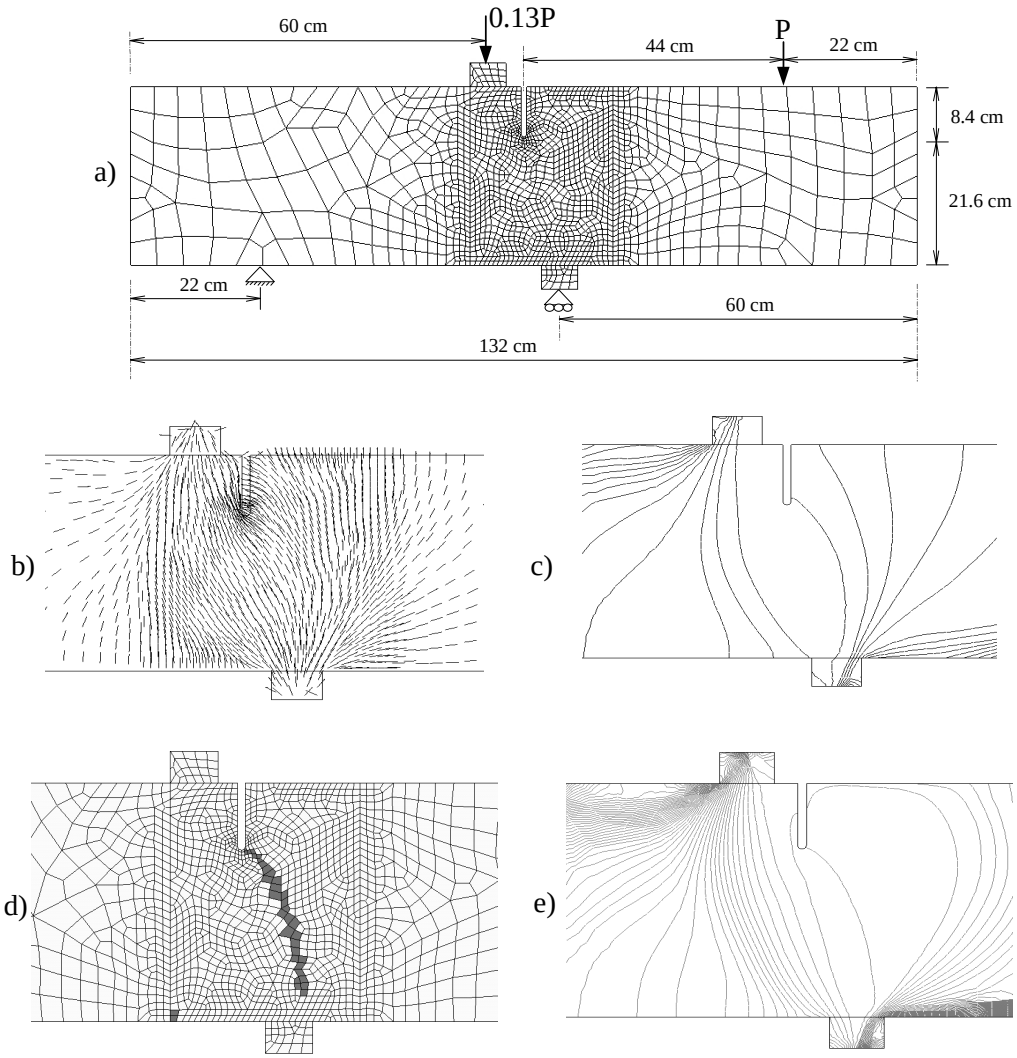

Figure 6: Application to a four points bending test

for all the meaningful values of θ_{S_i} are tangent at each point $\mathbf{x} \in \Omega$ to vectors $\mathbf{S}$ and $\mathbf{T}$. Therefore:

$$\left.\begin{array}{l} \mathbf{S}\cdot\nabla\theta = \nabla\theta\cdot\mathbf{S} = \frac{\partial\theta}{\partial S} = 0 \\ \mathbf{T}\cdot\nabla\theta = \nabla\theta\cdot\mathbf{T} = \frac{\partial\theta}{\partial T} = 0 \end{array}\right\} \quad in\ \ \Omega \tag{16}$$

Solutions of problem (16) are also solutions of the following heat conduction problem:

$$\begin{array}{lll} FIND: \theta(\mathbf{x}) & \text{satisfying:} & \\ & & \\ \nabla\cdot\mathbf{q} = 0 & in\ \ \Omega & (a) \\ \mathbf{q} = -\mathbb{K}\cdot\nabla\theta = -\mathbf{S}\frac{\partial\theta}{\partial S} - \mathbf{T}\frac{\partial\theta}{\partial T} & in\ \ \Omega & (b) \\ \mathbf{q}\cdot\nu = (\nu\cdot\mathbf{S})\frac{\partial\theta}{\partial S} + (\nu\cdot\mathbf{T})\frac{\partial\theta}{\partial T} = 0 & on\ \ \partial_q\Omega & (c) \\ \theta = \theta^* & on\ \ \partial_\theta\Omega & (d) \end{array} \tag{17}$$

where the anisotropic conductivity tensor $\mathbb{K}$ is given by:

$$\mathbb{K}(\mathbf{S}(\mathbf{x}),\mathbf{T}(\mathbf{x})) = \mathbf{S}\otimes\mathbf{S} + \mathbf{T}\otimes\mathbf{T} \tag{18}$$

and the introduction of an artificial conductivity ϵ leads to:

$$\mathbb{K}_\epsilon = \mathbf{S}\otimes\mathbf{S} + \mathbf{T}\otimes\mathbf{T} + \epsilon\mathbf{1} \tag{19}$$

The finite element discretization of problem (17) follows the steps of section 4 and the temperatures have to be prescribed at, at least, two points to obtain meaningful solutions. Once the temperature field $\theta(\mathbf{x})$ is determined at every node of the finite element mesh, a local (at elemental level) algorithm, the straightforward extension of the one in equation (3) to 3D cases, allows to determine the exact position of the discontinuity path inside every element.

5.1 3D representative simulation

Now the algorithm is applied to the case of a normal field $\mathbf{N}(\mathbf{x})$ oriented in the radial direction of a cube (see figure 7) with the origin at vertex O. That normal field is then:

$$\begin{array}{l} \mathbf{N}(\mathbf{x}) = \frac{\mathbf{x}}{|\mathbf{x}|} \\ \\ [\mathbf{N}(\mathbf{x})] = [n_x, n_y, n_z]^T \end{array} \tag{20}$$

from which a couple of tangent vectors, $\mathbf{S}$ and $\mathbf{T}$, can be immediately extracted as:

$$\begin{array}{l} [\mathbf{S}(\mathbf{x})] = [0, n_z, -n_y]^T \\ \\ [\mathbf{T}(\mathbf{x})] = [n_z, 0, -n_x]^T \end{array} \tag{21}$$

In figure 7-(a) the considered finite element mesh consisting of 1489 tetrahedra is presented. In 7-(b) the isothermal surfaces are plotted together with the prescribed temperatures. Notice that, as expected, the envelopes are spherical surfaces centered at vertex O.

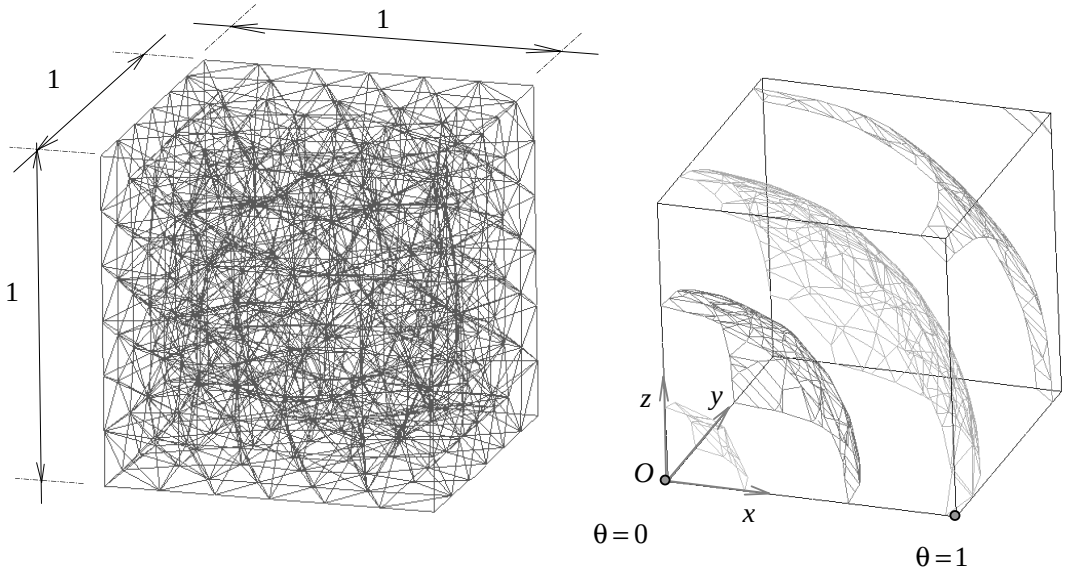

Figure 7: 3D envelops for a radial normal field.

6 Conclusions

In this work a global algorithm for tracking strong discontinuities has been presented. The assimilation of such an algorithm to a heat conduction problem provides some advantages, i.e.:

- Supplies a physical perception of the algorithm behaviour.
- Leads to a trivial implementation in finite element codes equipped with a thermal analysis module.

The resulting tracking methodology presents, in the authors' opinion, some advantages in front of the classical local tracking, namely:

- Once the nodal temperatures are known the algorithm (3), devoted to finding the discontinuity path inside a finite element, can be implemented at a pure elemental level.
- The algorithm's simplicity makes it a suitable candidate for multicracking problems were the discontinuity paths management requires robust and reliable tracking algorithms.
- For 3-D problems the proposed methodology contributes to substantially alleviate the huge topological difficulties posed by local tracking algorithms in three dimensional settings.

Acknowledgments

The authors wish to thank Prof. Sergio Idelsohn, from CIMEC Argentina, for some very helpful and illustrative comments on the topic of this work.

Financial support from the Spanish Ministry of Science and Technology through grant MAT2001-3863-C03-03 is gratefully acknowledged.

References

[1] F Armero and K. Garikipati. An analysis of strong discontinuities in multiplicative finite strain plasticity and their relation with the numerical simulation of strain localization in solids. *Int. J. Solids and Structures*, **33**, (20-22), 2863-2885, 1996.

[2] T. Belytschko, N. Moes, S. Usui, and C. Parimi. Arbitrary discontinuities in finite elements. *Int. J. Numer. Meth. Engng.*, (50), 993-1013, 2001

[3] E. Dvorkin, A. Cuitino, and G. Gioia. Finite elements with displacement embedded localization lines insensitive to mesh size and distortions. *Int. J. Num. Meth. Engng.*, **30**, 541-564, 1990.

[4] H. Lofti and P. Shing. Embedded representation of fracture in concrete with mixed finite elements. *Int. J. Numer. Meth. Engng.*, **38**, 1307-1325, 1995.

[5] J. Oliver, M. Cervera, and O. Manzoli. Strong discontinuities and continuum plasticity models: The strong discontinuity approach. *International Journal of Plasticity*, **15**, (3), 319-351, 1999.

[6] J. Oliver, A. Huespe, M. Pulido, and E. Chaves. From continuum mechanics to fracture mechanics: the strong discontinuity approach. *Engineering Fracture mechanics*, **69**, (2), 113-136, 2002.

[7] J. Oliver and J. Simo. Modelling strong discontinuities by means of strain softening constitutive equations. In H.M. et. al., editor, *Proc. EURO-C 1994 Computer Modeling of concrete structures*, pages: 363-372, Pineridge Press, Swansea, 1994.

[8] J. Oliver. Modeling strong discontinuities in solid mechanics via strain softening constitutive equations. Part 1: Fundamentals. *Int. J. Num. Meth. Engng.*, **39**, (21), 3575-3600, 1996

[9] J. Oliver. Modeling strong discontinuities in solid mechanics via strain softening constitutive equations. Part 2: Numerical simulation. *Int. J. Num. Meth. Engng.*, **39**, (21), 3601-3623, 1996

[10] K. Runesson, N.S. Ottosen, and D. Peric. Discontinuous bifurcations of elastic-plastic solutions at plane stress and plane strain *Int. J. of Plasticity*, **7**, 99-121, 1991.

[11] R. Regueiro and R. I. Borja. Plane strain finite element analysis of presure sensitive plasticity with strong discontinuity. *International Journal of Solids and Structures*, (38), 3647-3672, 2001.

[12] J. Simo and J. Oliver. A new approach to the analysis and simulation of strong discontinuities. In Z.B. et al., editor, *Fracture and Damage in Quasi-brittle Structures*, pages 25-39, 1994. E&FN Spon.

[13] J. Simo, J. Oliver, and F. Armero. An analysis of strong discontinuities induced by strain-softening in rate-independent inelastic solids. *Computational Mechanics*, **12**, 277-296, 1993.

[14] G. Wells and L. Sluys. A new method for modelling cohesive cracks using finite elements. *Int. J. Numer. Meth. Engng.*, (50), 2667-2682, 2001.

[15] K. Willam. Constitutive models for materials. In *Encyclopedia of Physical Science and Technology* (3^{rd} edition). Academic Press.

[16] A. Kobayashi, M. Hawkins, D. Barker, and B. Liaw. Frature process zone of concrete. In S.S.P., editor, *Application of Fracture Mechanics to Cementitious Composites*, pages 25-50. Marinus Nujhoff Publ., Dordrecht, 1985.

[17] O. Zienkiewicz and R. Taylor. *The Finite Element Method*. Butterworth-Heinemann, Oxford, UK, 2000.